

ORIGINAL ARTICLE

Improvement of histone deacetylase inhibitor efficacy by SN38 through TWIST1 suppression in synovial sarcoma

Satoru Sasagawa¹  | Jun Kumai² | Toru Wakamatsu³  | Yoshihiro Yui²

¹Molecular Biology Laboratory, Research Institute, Nozaki Tokushukai Hospital, Daito, Osaka, Japan

²Sarcoma Treatment Laboratory, Research Institute, Nozaki Tokushukai Hospital, Daito, Osaka, Japan

³Department of Musculoskeletal Oncology Service, Osaka International Cancer Institute, Osaka, Japan

Correspondence

Satoru Sasagawa, Molecular Biology Laboratory, Research Institute, Nozaki Tokushukai Hospital, Tanigawa 2-10-50, Daito, Osaka 574-0074, Japan.

Email: satoru.sasagawa@tokushukai.jp

Funding information

Japan Society for Promotion of Science, Grant/Award Numbers: 18K09051, 21K09338; Children's Cancer Association of Japan (2022)

Abstract

Background: Synovial sarcoma (SS) is an *SS18-SSX* fusion gene-driven soft tissue sarcoma with mesenchymal characteristics, associated with a poor prognosis due to frequent metastasis to a distant organ, such as the lung. Histone deacetylase (HDAC) inhibitors (HDACis) are arising as potent molecular targeted drugs, as HDACi treatment disrupts the SS oncoprotein complex, which includes HDACs, in addition to general HDACi effects. To provide further molecular evidence for the advantages of HDACi treatment and its limitations due to drug resistance induced by the microenvironment in SS cells, we examined cellular responses to HDACi treatment in combination with two-dimensional (2D) and 3D culture conditions.

Methods: Using several SS cell lines, biochemical and cell biological assays were performed with romidepsin, an HDAC1/2 selective inhibitor. SN38 was concomitantly used as an ameliorant drug with romidepsin treatment. Cytostasis, apoptosis induction, and MHC class I polypeptide-related sequence A/B (MICA/B) induction were monitored to evaluate the drug efficacy. In addition to the conventional 2D culture condition, spheroid culture was adopted to evaluate the influence of cell-mass microenvironment on chemoresistance.

Results: By monitoring the cellular behavior with romidepsin and/or SN38 in SS cells, we observed that responsiveness is diverse in each cell line. In the apoptotic inducible cells, co-treatment with SN38 enhanced cell death. In nonapoptotic inducible cells, cytostasis and MICA/B induction were observed, and SN38 improved MICA/B induction further. As a novel efficacy of SN38, we revealed TWIST1 suppression in SS cells. In the spheroid (3D) condition, romidepsin efficacy was severely restricted in TWIST1-positive cells. We demonstrated that TWIST1 downregulation restored romidepsin efficacy even

Abbreviations: DMEM, Dulbecco's modified Eagle medium; FBS, fetal bovine serum; HDAC, histone deacetylases; HDACi, HDAC inhibitor; MICA/B, MHC class I polypeptide-related sequence A/B; NK, natural killer; qRT-PCR, quantitative real-time polymerase chain reaction; SS, synovial sarcoma; ULBPs, UL16 binding proteins.

This is an open access article under the terms of the [Creative Commons Attribution-NonCommercial](https://creativecommons.org/licenses/by-nc/4.0/) License, which permits use, distribution and reproduction in any medium, provided the original work is properly cited and is not used for commercial purposes.

© 2024 The Authors. *Cancer Innovation* published by John Wiley & Sons Ltd on behalf of Tsinghua University Press.

in spheroid form, and concomitant SN38 treatment along with romidepsin reproduced the reaction.

Conclusions: The current study demonstrated the benefits and concerns of using HDACi for SS treatment in 2D and 3D culture conditions and provided molecular evidence that concomitant treatment with SN38 can overcome drug resistance to HDACi by suppressing TWIST1 expression.

KEYWORDS

HDAC inhibitor, MICA/B, SN38, spheroid, synovial sarcoma, TWIST1

1 | INTRODUCTION

Synovial sarcoma (SS) is one of the rare aggressive malignancies with a poor prognosis due to frequent metastasis to distant organs, such as the lungs and liver [1, 2]. It mainly occurs in adolescents and young adults. SS is characterized by the *SS18-SSX1/2/4* fusion genes derived from t(X;18) (p11.2; q11.2) translocation [1, 2]. The chimeric oncoprotein therefrom has been reported to hijack BRG1- or BRM-associated factor (BAF, also known as mSWI/SNF) chromatin remodeling complex and exert an oncogenic activity [3, 4]. In the current study, it was etiologically thought that SS18-SSX containing BAF complex broadly reprograms transcriptional regulation, resulting in the initiation and progression of SS tumors [3, 4]. Therefore, the *SS18-SSX* fusion gene or its product has been regarded as a critical molecular target for SS treatment; however, despite several attempts, SS18-SSX targeted therapy has remained a challenge or is still considered undruggable [5].

In current SS therapies, doxorubicin and ifosfamide are administered in combination with surgery and radiation [6]. However, due to their limited benefits, the risk for recurrence and metastases in patients with SS remains. In particular, higher drug resistance at the metastatic site makes treatment difficult, resulting in poor prognosis. Thus, additional drugs to treat SS would be required. Histone deacetylase (HDAC) inhibitors (HDACis) are prominent antitumor drugs owing to their diverse effects, including cell-cycle arrest, senescence, and apoptosis in both normal and tumor cells [7–9]. For SS treatment, an HDACi is considered one of the optimal drug candidates, because a recent study has reported HDAC to form a transcriptional complex with SS18-SSX [10]. The SS18-SSX molecule can bind to the activating transcription factor 2 (ATF2) and recruit Polycomb group components, including HDAC, to ATF2 target promoters via transducin-like enhancer of split 1, resulting in the repression of ATF2 target genes, such as tumor suppressors, including early growth response 1, and activating

transcription factor 3 (ATF3). Indeed, a transcriptomic study for HDACi in SS cells explained, in detail, that HDAC inhibition induced upregulation of the cytostatic factor, accumulation of ROS leading to reduction of antioxidant factors (SOD1, 2), induction of immunological antigen, including natural killer (NK) ligands MHC class I polypeptide-related sequence A/B (MICA/B) and UL16 binding proteins (ULBPs), and upregulation of apoptotic factors, such as BIK, thereby directing orchestrated cell death [9]. Recent studies have suggested the importance of natural killer cell immune surveillance in soft tissue sarcoma suppression [11–14]; thus, MICA/B and ULBPs induction properties of HDACi are particularly noteworthy in this regard. However, despite the valuable evidence from biomedical studies, no HDACi has been approved for SS treatment yet.

The tumor microenvironment is a complex system. Tumor cells are subjected to physical, chemical, and biochemical influences, resulting in the promotion of cell growth, differentiation, invasion, and drug resistance [15, 16]. Historically, drug discovery screening has been performed in two-dimensional (2D) adherent culture conditions. In such conventional conditions, the cells are isolated, morphologically flattened, and are considered to have altered intracellular functions, such as signaling network, metabolism, and gene regulation, compared to those in tumor tissues in patients. Thus, 2D culture conditions are concerned to be an oversimplified condition for drug screening [17, 18]. To better reflect patients' tumor condition in vitro, cell mass culture systems (3D culture conditions), such as spheroids from the cell lines and tumor organoids directly from patients' tumors, have been studied in detail [18–20]. In 3D culture, the architecture of cell–cell and cell–matrix interactions are retained, and soluble factors, including oxygen, nutrients, and low-molecular-weight chemicals, are diffused along a concentration gradient. Indeed, drug screening with cancer tissue-originated spheroid, a kind of tumor organoid culture system, demonstrated higher drug resistance than that in 2D culture and patient-dependent responsibility [21–23].

Thus, the 3D culture system is increasingly getting recognized as better suited for drug testing, since the conditions reflect more physiological cellular circumstances in the tumor tissue.

TWIST1, a basic helix-loop-helix transcription factor, is known to play crucial roles both in normal and tumor conditions [24]. During embryogenesis, *Twist1* appears in the neural crest (NC) and triggers cell migration from there by suppressing E-cadherin [25]. It is also known to be a key player in the stemness of mesenchymal stem cells [24]. In carcinoma, TWIST1 functions as an epithelial-to-mesenchymal transition (EMT) factor and promotes metastasis through the upregulation of multiple cellular functions, such as motility, anoikis resistance, invadopodia formation, and induction of matrix-metalloproteases [24, 26]. In addition, TWIST1 has been shown to be one of the key players in drug resistance against paclitaxel, cisplatin, and fluorouracil, although its detailed mechanism is not fully understood yet [27]. Therefore, TWIST1 is considered a crucial molecular target in chemotherapy. In colorectal cancer, TWIST1 expression was found to be correlated with metastatic activity [28, 29]. Irinotecan and its active metabolite form, SN38, have been studied as a key chemotherapeutic drug for metastatic colorectal cancer [30]. In the mouse model of osteosarcoma, lung metastasis of LM8 cells was inhibited by irinotecan [31]. Interestingly, the LM8 cell was reported to be TWIST1-positive and its parental cell line Dunn was TWIST1-negative (our unpublished data). The data suggested the possibility of irinotecan/SN38 competing with TWIST1.

The function and regulation of TWIST1 in sarcoma cells have been less investigated than in carcinoma cells. One of the cell-of-origin of SS is suspected to be the migrating mesenchymal cell from NC triggered by TWIST1 expression since SS tends to develop in soft tissues derived from NC cell lineages, such as ligaments and muscles around the joint tissue in the arms and legs [1, 2]. Consistent with this fact, some of the SS cell lines were shown to have mesenchymal differentiation properties [32–35]. TWIST1 has also been shown to play crucial roles in maintaining mesenchymal state and tumor initiation properties in SS cells [36]; therefore, TWIST1 is thought to be a pivotal molecule, although its function and regulation in SS cells are yet to be fully understood.

In this study, we observed diverse responses, including drug resistance in response to HDACi treatment, in 2D and 3D culture systems; TWIST1 expression may be responsible for the cause of HDACi resistance, especially in 3D culture conditions. In addition, we reported TWIST1 expression in SS cells to be suppressed by SN38, leading to the re-establishment of HDACi efficacy even under 3D culture conditions.

2 | MATERIALS AND METHODS

2.1 | Chemicals and reagents

Romidepsin and trichostatin A (TSA; #58880-19-6) were obtained from Cayman Chemical Co., SN38 was purchased from Tocris Bioscience, poly-(2-hydroxyethyl methacrylate) (poly-HEMA; #P3932) was procured from Sigma-Aldrich, and PEI-MAX (M.W. 40000) (#24765-100) was from Polysciences. Other general chemicals and reagents were purchased from FUJIFILM Wako Pure Chemical Industries, Sigma-Aldrich, or Nacalai Tesque.

2.2 | Cells

Aska-SS and Yamato-SS cell lines were gifted by Dr. Norifumi Naka. HSSYII cell line was obtained from RIKEN Cell Bank. SYO1 cell line was kindly provided by Dr. Akira Kawai. The cells were maintained in Dulbecco's modified Eagle medium (DMEM) supplemented with 10% (SYO1 and HSSYII) or 20% (Aska and Yamato) fetal bovine serum (FBS) at 37°C in 5% CO₂ and 100% humidity. The 293FT cell line was purchased from Thermo Fisher Scientific; they were maintained in DMEM containing 10% FBS, 2 mM L-glutamine, sodium pyruvate, and nonessential amino acids at 37°C in 5% CO₂ and 100% humidity.

2.3 | Quantitative RT-PCR analysis

Total RNA was purified with TRIzol reagent and cDNA was prepared using the PrimeScript RT Reagent Kit (#RR037; Takara Bio). Quantitative RT-PCR was performed using the TB Green Premix Ex Taq II (#RR820; TaKaRa Bio) and gene-specific primer pairs in the CFX96 Touch Real-time PCR system (Bio-Rad Laboratories). Sequences of the primer pair (Supporting Information: Table 1) were obtained from the PrimerBank database (<https://pga.mgh.harvard.edu/primerbank/index.html>).

2.4 | Hypoxic cultures

Hypoxia was generated using the BIONIX-1 hypoxic culture kit (Sugiyamagen) with an oxygen absorber (AneroPack-Aneaero; Mitsubishi Gas Chemical), according to the manufacturer's protocol. The pO₂ levels were monitored with an oxygen concentration monitor (OXY-1; JIKCO). The hypoxically cultured SS cells were immediately cooled down on ice and lysed with

ice-cold RIPA buffer to obtain whole-cell lysates or with TRIzol (#11596) (Thermo Fisher Scientific) for RNA extraction.

2.5 | Spheroid cultures

The poly-HEMA-coated dishes were prepared as described previously [34]. To allow spheroid formation, the trypsinized cells were spread onto 10-cm poly-HEMA-coated dishes with 15 mL of culture medium, and the culture continued for up to 7 days. During spheroid formation, the culture medium was replaced every 2 days. For each assay, spheroids were transferred into new 6-cm poly-HEMA-coated dishes with 5 mL of fresh culture medium containing the drugs of interest.

2.6 | Western blot analysis

Antibodies used for western blot analysis are as follows: anti-MICA/B (#sc137242, 1:200; Santa Cruz Biotechnology), anti-Twist1 (#sc81417, 1:500; Santa Cruz Biotechnology), anti-MHC I (#sc55582, 1:500; Santa Cruz Biotechnology), anti-HIF1 α (#610958, 1:1000; BD Biosciences), anti-acetyl-histone H3 (Lys9) (#9649, 1:1000; Cell Signaling Technology), and anti- β -actin (#sc47778, 1:1000; Santa Cruz Biotechnology). Horseradish peroxidase-conjugated anti-mouse IgG (#115-035-146, 1:2500) and anti-rabbit IgG (#711-035-152, 1:2500) were purchased from Jackson ImmunoResearch. Western blot analysis was performed according to the standard protocol described previously [37].

2.7 | Immunofluorescence and TUNEL assay

The spheroid was fixed with 10% formalin at 4°C and embedded in paraffin according to the standard protocol. The paraffin block was sectioned at 8- μ m thickness using a microtome (Leica). Following deparaffinization, the samples were incubated overnight in 20 mM Tris-HCl (pH 9.0) at 70°C to retrieve the antigens. The samples were treated with blocking reagent (Roche) solution (1%) for 30 min and then stained with primary antibodies of interest in a moist box at 4°C, overnight, followed by Alexa 555-conjugated secondary antibody (ab150106, 1:500; Abcam) staining for 2 h at room temperature. The TUNEL assay was performed with in situ cell death detection kit (Sigma-Aldrich), according to the manufacturer's protocol. The nuclei were counterstained with Hoechst 33342 (1:1000; Thermo Fisher Scientific). The

fluorescent images were visualized and captured using the Eclipse Ti fluorescence microscope (Nikon) and NIS-elements software (Nikon).

2.8 | Plasmid construction and lentivirus generation

shRNA expression backbone vector pLKO.1puro plasmid (#8453) was provided by Dr. Bob Weinberg via Addgene [38]. The *TWIST1* shRNAs were designed using the Biosettia tool (<https://biosettia.com/>). The target sequence oligos (Supporting Information: Table 1) were annealed and inserted into the pLKO.1 puro plasmid according to the protocol provided by Addgene. A lentiviral packaging mixture (pLP1, pLP2, and pLP/VSVG) was purchased from Thermo Fisher Scientific. Lentivirus generation, infection, and selection by puromycin were performed as described previously [39].

2.9 | Statistical analyses

All quantitative results are presented as the mean \pm standard deviation, unless specified otherwise. Group pairs were compared by performing the two-tailed unpaired Student's *t*-test in Microsoft Excel (Microsoft), and the Statcel3 add-in was used in Excel (OMS Publishing). Statistical significance was set as $p < 0.05$.

3 | RESULTS

3.1 | HDAC expression profile and cellular response to HDAC inhibition

A previous transcriptomic study revealed the systematic efficacy of HDACi treatment in SS cells [9]. To further analyze the cellular response of SS cells to HDACi, four SS cell lines (Aska [biphasic, *SS18-SSX1*], Yamato [biphasic, *SS18-SSX1*], SYO1 [biphasic, *SS18-SSX2*], and HSSYII [monophasic, *SS18-SSX1*]) were examined. To see the distribution of the HDAC family across SS cell lines, quantitative real-time polymerase chain reaction (qRT-PCR) analysis was performed (Figure 1a). *HDAC2* was found to be predominantly expressed followed by *HDAC1*, and the expression patterns were very similar across the cell lines. To examine the cellular response to HDAC inhibition, the SS cells were treated with romidepsin, a potent HDAC1/2-selective HDACi, under adherent culture (2D) conditions. A lower concentration (20 nM) of romidepsin was employed for the experiments, judged by the induction of histone acetylation accumulation and the plateau of

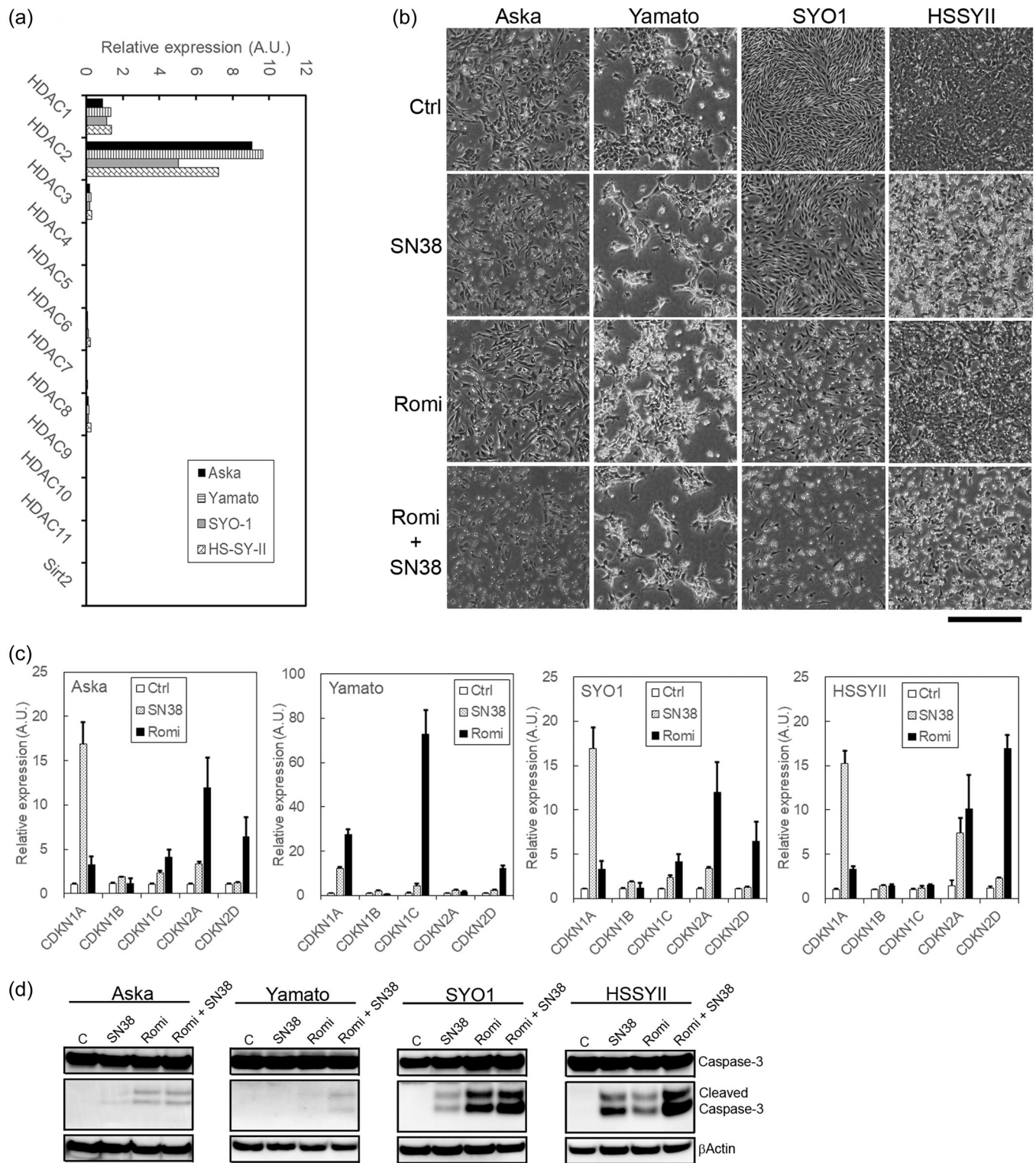


FIGURE 1 Differences in responsiveness among SS cell lines to romidepsin and SN38. (a) Expression profile of the HDAC family among SS cell lines. mRNA of the HDAC family was semiquantitatively observed by qRT-PCR. Expression of *HPRT1* was used as an internal standard and normalized with respect to *HDAC1* expression in Aska. (b) SS cells were treated with SN38 (1 μ M), romidepsin (20 nM), or both for 24 h. (c) qRT-PCR results of cyclin-dependent kinase inhibitors after treatment of romidepsin (20 nM) or/and SN38 (1 μ M) for 24 h. Expression of *hpri1* was used as an internal standard. (d) Cleaved Caspase3 at 24 h posttreatment of romidepsin (20 nM) or/and SN38 (1 μ M). The scale bar in (b) represents 200 μ m. HDAC, histone deacetylase; SS, synovial sarcoma.

MICA/B induction to avoid excess side effects (Supporting Information: Figure 1a). Here, SN38 was used as a concomitant drug, because we found it to suppress the expression of TWIST1, as shown below (Figure 3).

Although romidepsin-induced cytostasis was observed in all cell lines, cytotoxicity was seldom seen in Yamato. On the other hand, significant cell death was observed in SYO1 and HSSYII (Figure 1b). SN38 induced cytotoxicity in Aska and HSSYII, and mild cell death in SYO1. qRT-PCR analysis for cyclin-dependent kinase inhibitors revealed that *CDKN1A* (p21/WAF) was predominantly induced by SN38 treatment while *CDKN2A* (p16/Ink4a) and *CDKN2D* (p19/Ink4d) were predominantly induced by romidepsin (Aska, SYO1, HSSYII), consistent with the findings of previous transcriptomic study [9]. While *CDKN1A* induction by SN38 was mild, *CDKN1C* (p57/Kip2), but not *CDKN2A/D*, was strongly induced in Yamato (Figure 1c). Monitoring of Caspase3 cleavage revealed that romidepsin or SN38 treatment can induce significant apoptosis in SYO1 and HSSYII, though not in Aska and Yamato (Figure 1d). Concomitant treatment of these drugs synergized apoptosis induction in SYO1 and HSSYII. Despite weak apoptosis induction caused by concomitant treatment, Aska cells seemed to have died (Figure 1b,d). A different cell death pathway might be activated in Aska. Overall, despite the similar HDAC expression profiles, cellular response to romidepsin and SN38 was different in each cell line. Although cytostasis by low-dose romidepsin was observed in all cell lines used, a significant cell death signature was observed in two of the four cell lines, suggesting limited direct cytotoxicity of romidepsin in SS cells.

3.2 | MICA/B induction by HDAC inhibition and its enhancement with SN38

The efficacy of HDAC inhibition is not only exerted by direct cytotoxicity but also by the induction of indirect cytotoxicity-related molecules. MICA/B, cell surface ligands recognized by NKG2D receptor on NK cells, have been reported to be induced by HDACi treatment in several tumor cells, including SS cells [9, 40–43]. We confirmed that romidepsin could induce MICA/B and IgG expression similar to TSA, a kind of pan-HDAC inhibitor (Supporting Information: Figure 1b). Thus, we monitored MICA/B induction as an index of HDAC inhibition efficacy by romidepsin. Among the cell lines used, MICA/B was naturally expressed only in Aska. Regardless of the initial state of MICA/B expression, romidepsin treatment induced MICA/B in all cell lines (Figure 2a). Although SN38 did not have MICA/B induction activity, concomitant treatment with romidepsin enhanced MICA/B induction in Yamato. In SYO1 and HSSYII, the

concomitant treatment seemed to rather reduce MICA/B expression at the protein level (Figure 2a). However, at the mRNA level, enhanced induction of *MICB*, due to concomitant treatment with SN38, was observed in both SYO1 and HSSYII as well as in Yamato cells (Figure 2b). Considering the cell death activity of these drugs in SYO1 and HSSYII, the cells were likely to die before the induced *MICA/B* mRNA was fully translated to the MICA/B protein. Note that MICA/B induction by romidepsin at the protein level was milder in Yamato, compared to that in Aska, despite the *MICB* induced by romidepsin in Yamato overcoming about twice that naturally induced in Aska (Figure 2c). Since TWIST1 is known to exhibit drug resistance activity in multiple ways, and all SS cell lines except Aska displayed strong TWIST1 expression (Figure 2d), we hypothesized that TWIST1 interrupted MICA/B expression. To confirm this idea, we adopted *TWIST1*-knockdown cells. Yamato cells were infected with sh*TWIST1*-expressing lentivirus and a significant reduction of TWIST1 expression was confirmed (Figure 2e). As expected, MICA/B induction by romidepsin was strengthened in *TWIST1*-knockdown cells (Figure 2f). Taken together, concomitant treatment of romidepsin with SN38 was found to enhance MICA/B induction, and TWIST1 could interrupt MICA/B expression induced by romidepsin in SS cells.

3.3 | TWIST1 suppression by SN38

As shown above, concomitant treatment with SN38 enhanced the effect of romidepsin on MICA/B induction. Moreover, TWIST1 downregulation improved MICA/B induction by romidepsin. Thus, we hypothesized that SN38 may suppress the function of TWIST1. To address this idea, at first, SS cells were treated with SN38, and TWIST1 expression was monitored. As expected, SN38 was found to suppress TWIST1 expression in Yamato (Figure 3a). Previous reports had demonstrated that STAT3 inhibitor and NF- κ B inhibitor could suppress TWIST1 expression in several carcinoma cells [44–46]; however, the drugs rather increased TWIST1 expression in Yamato. Meanwhile, romidepsin treatment did not affect TWIST1 expression (Figure 3b). To further confirm that suppression of TWIST1 by SN38 is common in all SS cell lines, SYO1 and HSSYII cells were treated with SN38 in a dose-dependent manner. Indeed, SN38 suppressed TWIST1 both in SYO1 and HSSYII (Figure 3c), indicating that TWIST1 suppression by SN38 was conserved across the SS cell lines. At the mRNA level, *TWIST1* expression was not reduced, and rather increased slightly in all cell lines tested (Figure 3d), thereby suggesting that TWIST1 suppression by SN38 was not due to transcriptional disruption but due to increased protein instability.

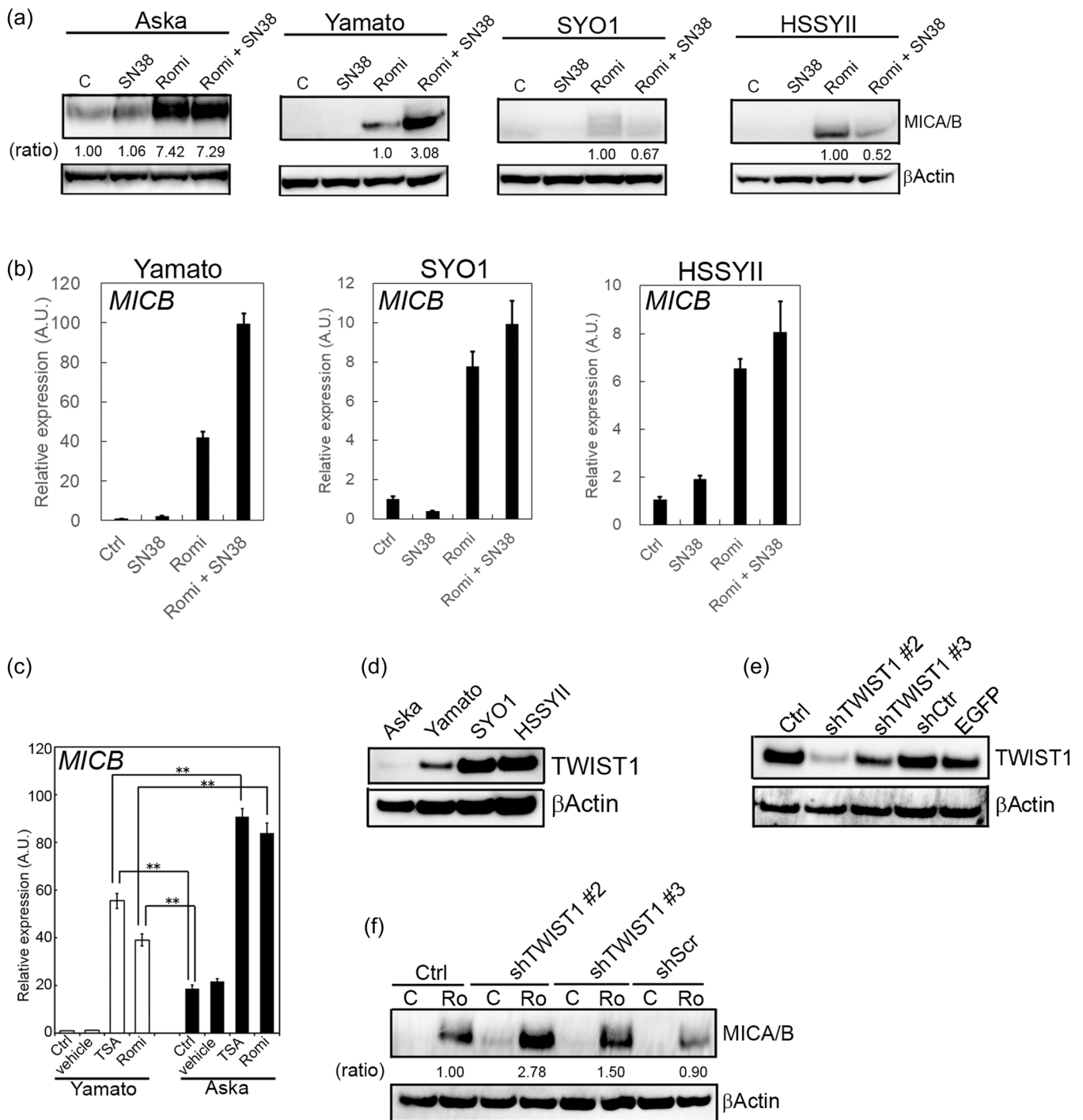


FIGURE 2 MICA/B induction by romidepsin and its suppression by TWIST1. (a) MICA/B induction at 24 h posttreatment of romidepsin (20 nM) or/and SN38 (1 μ M) was monitored by western blot analysis. Expression strength was normalized with the corresponding β Actin band. Note that the significant spontaneous MICA/B expression was detected in AskA. (b) qRT-PCR results of *MICB* induction after treatment of romidepsin (20 nM) or/and SN38 (1 μ M) for 24 h. Expression of *HPRT1* was used as an internal standard. (c) Comparison of *MICB* induction by HDACi (TSA; 1 μ M, romidepsin; 20 nM) between AskA and Yamato. Expression of *HPRT1* was used as an internal standard and normalized with respect to *MICB* expression in Yamato. (d) Expression profile of TWIST1 by western blot analysis among SS cell lines. (e) Result of *TWIST1* knockdown by sh*TWIST1* lentivirus infection. Yamato cells were infected with lentivirus carrying indicated shRNA and the infected cells were selected with puromycin. (f) MICA/B induction by romidepsin (20 nM) in sh*TWIST1* expressed Yamato cells. Expression strength was normalized with the corresponding β Actin band. Statistical significance was determined by Student's *t*-test. ***p* < 0.01. HDAC, histone deacetylase; MICA/B, MHC class I polypeptide-related sequence A/B; SS, synovial sarcoma; TSA, trichostatin A.

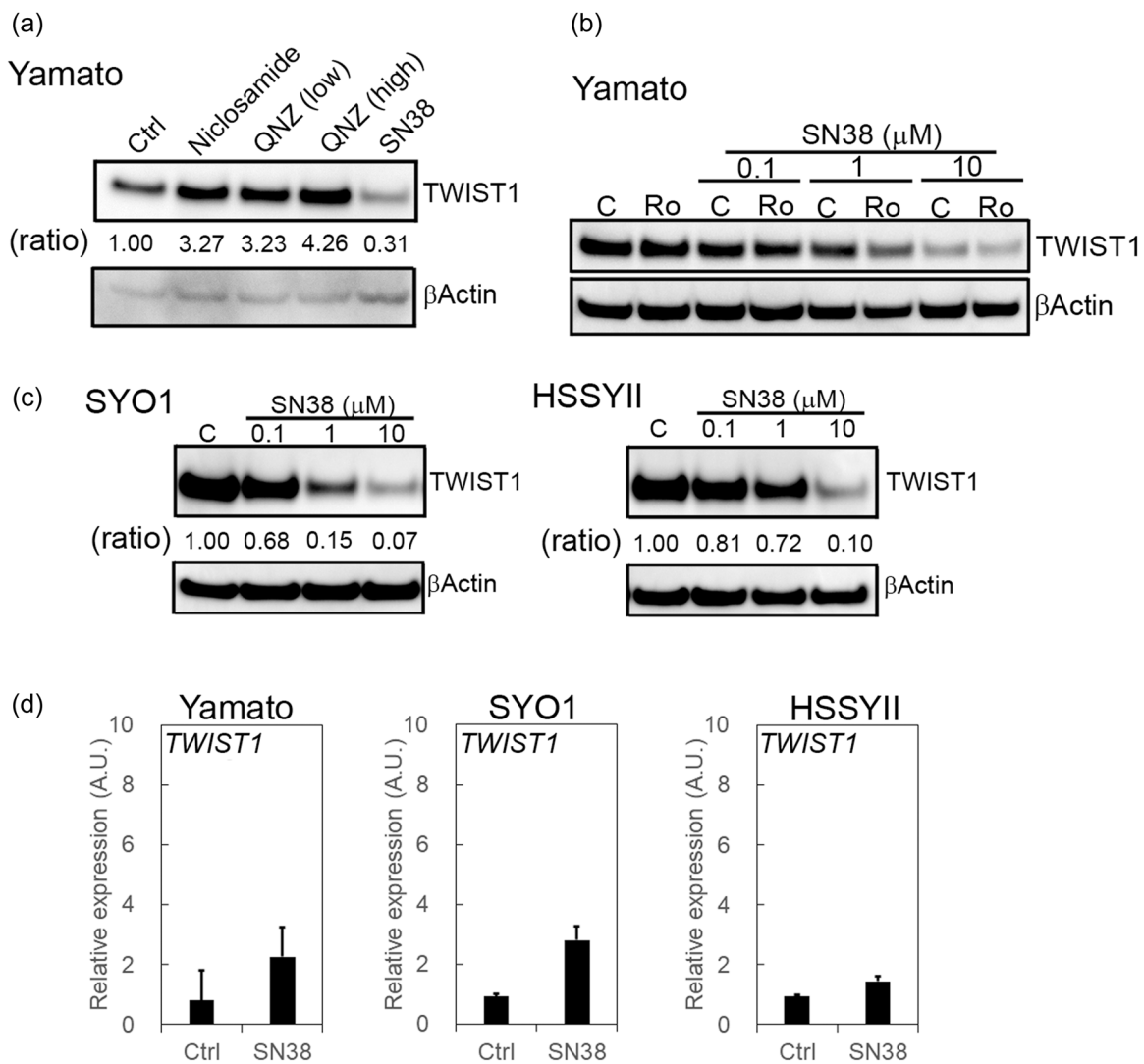


FIGURE 3 TWIST1 suppression by SN38. (a) Yamato cells were treated with Niclosamide (2 μM), QNZ (1 or 10 μM), or SN38 (10 μM) for 24 h and TWIST1 expression was monitored by western blot analysis. The expression strength of TWIST1 was normalized with the corresponding βActin band. (b) Yamato cells were treated with SN38 at the indicated concentration without or with romidepsin (20 nM) for 24 h. C and Ro represent control (no treatment) and romidepsin, respectively. (c) SYO1 and HSSYII were treated with SN38 at the indicated concentrations for 24 h. The expression strength of TWIST1 was normalized with the corresponding βActin band. (d) qRT-PCR results of *TWIST1* expression at 24 h posttreatment of romidepsin (20 nM). Expression of *HPRT1* was used as an internal standard.

3.4 | Hypoxia in spheroids and limitations of HDACi efficacy

Currently, 3D culture systems, such as spheroids and organoids, are shedding light owing to their drug responsiveness being similar to that of tumor tissue in patients [17–20]. Various cellular functions are known to be altered, and cell-mass autonomous microenvironments, such as hypoxia, are known to appear in 3D conditions. To dissect what happened in SS spheroids, immunofluorescence was adopted. Indeed, a hypoxic area indexed by HIF1α expression was observed inside the Yamato spheroid (Figure 4a, middle). Since *TWIST1* is a direct transcriptional target of HIF1α, its upregulation was detected in the matching area

inside the spheroid (Figure 4a, bottom). Further, since TWIST1 is known to have antiapoptotic activity, the cells in the hypoxic area seemed to better withstand apoptosis induction in the Yamato spheroid than in the Aska spheroid, as indicated by TUNEL staining (Figure 4b, bottom). On the other hand, remarkable HIF1α stabilization was not observed in the Aska spheroid (Figure 4a, top), and apoptotic cells were detected from the shallow layer (Figure 4b, top). Under hypoxia in 2D culture condition, TWIST1 upregulation was observed in Yamato but not in Aska (Figure 4c). Considering the induction of *VEGF* mRNA, another direct HIF1α target, it was found to be well induced in 2D hypoxia, although not significant in Aska spheroids (Figure 4d); this indicated that Aska cells were still responsive to the hypoxic

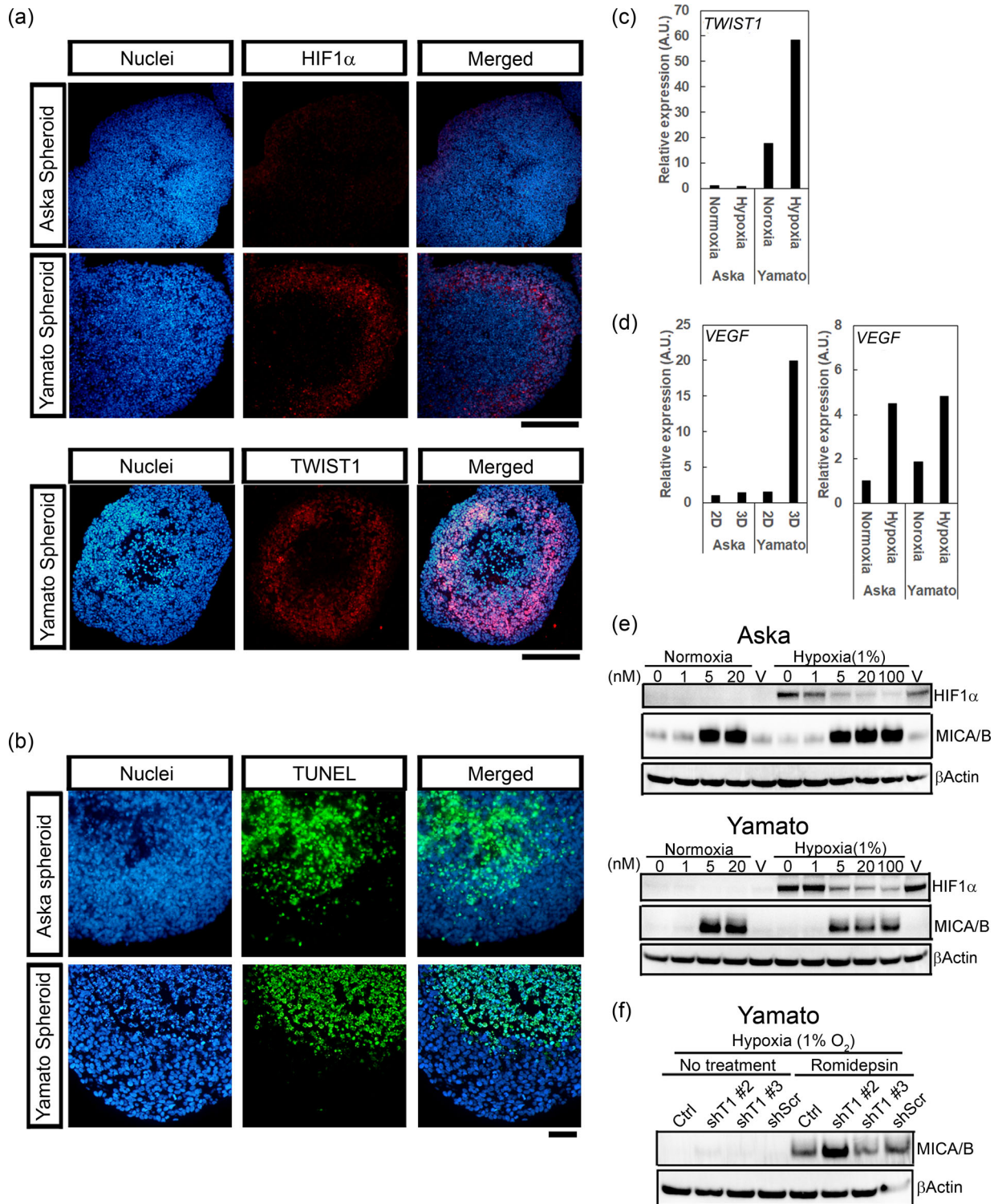


FIGURE 4 Enhanced romidepsin resistance triggered by TWIST1-related microenvironments. (a) Immunofluorescent staining of HIF1 α and TWIST1 in Aska and Yamato spheroids. (b) Immunofluorescent results of TUNEL assay in Aska and Yamato spheroids. (c) qRT-PCR results of *TWIST1* induction in Aska and Yamato under hypoxia condition for 48 h. Expression of *HPRT1* was used as an internal standard. (d) Comparison of qRT-PCR results of *VEGF* induction between 2D and 3D condition (left) or between under normoxia and hypoxia in Aska and Yamato cells (right). Expression of *HPRT1* was used as an internal standard. (e) Comparison of MICA/B induction by romidepsin at the indicated concentration (nM) between under the normoxia and hypoxia at the 2D condition in Aska (top) and Yamato (bottom) cells. (f) MICA/B induction by romidepsin (20 nM) under the hypoxia 2D culture condition in sh*TWIST1*-expressing Yamato cells. The scale bars in (a) and (b) represent 200 μ m and 50 μ m, respectively. MICA/B, MHC class I polypeptide-related sequence A/B.

condition, suggesting that *TWIST1* in Aska cells was epigenetically silenced. Collectively, cell-mass autonomous hypoxia seemed to be hard to maintain in *TWIST1*-negative Aska spheroids. To further address the effect of hypoxia on the efficacy of HDACi, SS cells were treated with romidepsin in a dose-dependent manner under hypoxic conditions. As expected, MICA/B was induced, even under hypoxia, to a similar extent as under normoxia, in *TWIST1*-negative Aska cells (Figure 4e, top). In contrast, MICA/B induction was limited under the hypoxic condition in *TWIST1*-positive Yamato cells (Figure 4e, bottom). This reduction was not restored by an increment of romidepsin concentration from 5 to 100 nM. HIF1 α stability was decreased by romidepsin in a dose-dependent manner, consistent with a previous report [47]. To check whether *TWIST1* knockdown rescued MICA/B induction even under hypoxia, sh*TWIST1*-expressing Yamato cells were treated with romidepsin under hypoxia, and the above was confirmed (Figure 4f). Taken together, hypoxia-induced *TWIST1* was considered to interrupt the efficacy of romidepsin.

3.5 | Restoration of HDACi efficacy by SN38 in spheroid form

The above data raised concerns regarding the limitation of the efficacy of HDACi in the 3D culture condition due to microenvironmental influences, such as hypoxia coordinated by *TWIST1*. The effect of romidepsin was severely restricted in the *TWIST1*-positive Yamato spheroid, as judged by an increment of Acetyl-H3 (Figure 5a, left). Consistently, MICA/B induction was found to be very weak. In contrast, romidepsin treatment was relatively effective in *TWIST1*-negative Aska spheroid (Figure 5a, right). To estimate romidepsin interruption efficacy at each culture condition, the induction of MICA/B protein and mRNA was semiquantitatively observed (Figure 5b). In Aska cells, romidepsin induced MICA/B expression to the same extent even under hypoxia, and approximately 80% in spheroid condition (Figure 5b, top-left). The mRNA induction of *MICA* was almost consistent with the protein result (Figure 5b, top-right). In Yamato cells, MICA/B expression was reduced to approximately 50% under hypoxia, and approximately 10% in spheroid condition, compared to that under 2D culture condition (Figure 5b, bottom-left). Similar to protein data, *MICA* mRNA induction was restricted under hypoxia and in spheroid conditions in approximately the same proportion (Figure 5b, bottom-right). Compared to that under hypoxia, the restriction of MICA/B induction was more severe in the spheroid condition in both cell lines. It suggested the existence of additional restriction mechanisms in the spheroid condition. Importantly, the severe restriction of

MICA/B induction by romidepsin in spheroid condition was restored in *TWIST1*-knockdown spheroid (Figure 5c), indicating *TWIST1* as a dominant interrupter of romidepsin in spheroid condition. The data raised the expectation that SN38 could release the interruption against romidepsin in spheroid form as well. To confirm the same, Yamato spheroid was treated with romidepsin accompanied by SN38. As expected, concomitant SN38 treatment restored the limited MICA/B induction by romidepsin in spheroid condition (Figure 5d, left). Moreover, the restoration of romidepsin efficacy by SN38 was confirmed at the *MICA* induction level (Figure 5d, right). Taken together, concomitant treatment of SN38 with romidepsin was expected to overcome the drug resistance triggered by cell-mass autonomous hypoxia mediated by *TWIST1*.

In summary, we demonstrated that romidepsin efficacy was restricted by *TWIST1*; however, it was restored by concomitant SN38 treatment via *TWIST1* suppression. The microenvironment in cell-mass condition could induce HDACi resistance through *TWIST1* upregulation. The combinatorial usage of these drugs overcame the restriction of HDACi in the spheroid condition, suggesting the potential of improving HDACi treatment in patients with SS (Figure 6). Our data encouraged the trial for HDACi accompanied by SN38/irinotecan in patients with SS.

4 | DISCUSSION

Chemotherapy for patients with SS using conventional cytotoxic drugs offers limited benefits and retains the risk of recurrence and metastasis. As SS18-SSX is known to form a complex with HDAC, HDACi is considered a prominent molecular targeted drug candidate for SS treatment. The milestone study of HDACi transcriptomic analysis in SS cells verified its orchestrated cytotoxic efficacy in SS cells [9]. Consistent with that report, our cellular and biochemical response-based analysis demonstrated similar efficacy of HDACi with diverse molecular responses. HDACi treatment induced cytostasis in all cell lines used, with different *CDKN* expression patterns, thereby suggesting that the character of the responsiveness of the cells against HDACi is not uniform. A definitive apoptotic response against romidepsin was observed only in SYO1 and HSSYII cells. Conversely, remarkable MICA/B induction was observed in Aska and Yamato cells. In the experimental context, MICA/B induction by HDACi could be seen as a compensational drive in case of dysfunction of apoptosis induction. Since the NK cell immunosurveillance system plays a pivotal role in the defense mechanism for sarcoma suppression, the MICA/B induction activity of

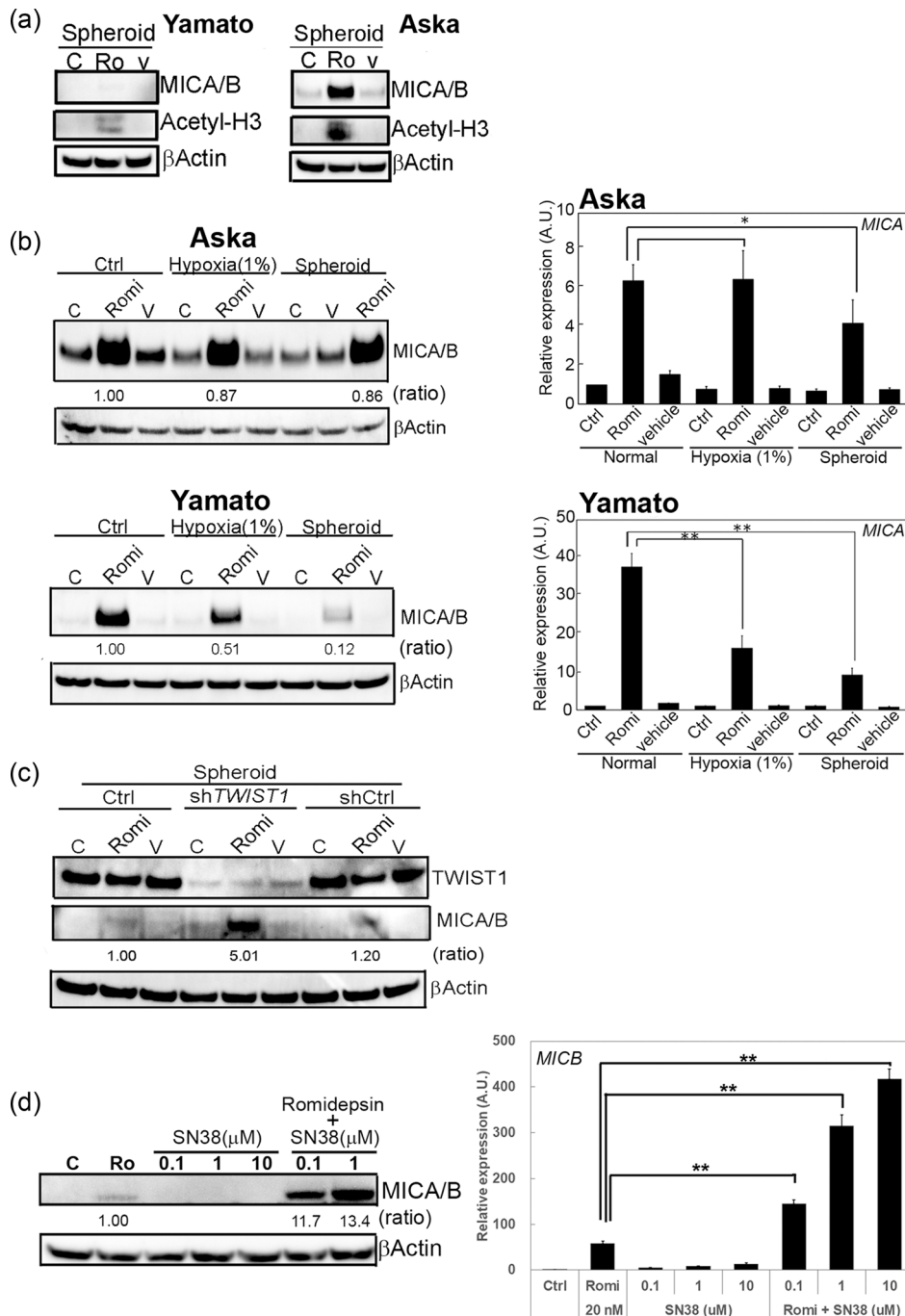


FIGURE 5 Restriction of romidepsin efficacy in spheroid and its restoration by SN38. (a) Monitoring of romidepsin efficacy on MICA/B induction in the spheroid form of Aska (right) and Yamato (left). Acetyl-H3 (Lys9) was observed as an index of HDAC inhibition. (b) Comparison of MICA/B induction efficacy of romidepsin (20 nM) for 24 h among normoxia, hypoxia, and spheroid conditions. The expression strength of MICA/B (left) was normalized with the corresponding β Actin band and that in normoxia was set as standard. The expression of *MICA* mRNA was semiquantified by qRT-PCR and normalized with respect to *MICA* expression under normoxia conditions. *HPRT1* was used as an internal standard. (c) sh*TWIST1*-expressing Yamato-spheroid was treated with romidepsin (20 nM) for 24 h. The expression strength of MICA/B was normalized with the corresponding β Actin band and that in parental Yamato-spheroid was set as standard. (d) Yamato-spheroid was treated with romidepsin (20 nM) without or with SN38 at the indicated concentration. The expression strength of MICA/B (left) was normalized with the corresponding β Actin band and that in romidepsin single treatment was set as standard. The expression of *MICB* (right) was semiquantified by qRT-PCR and normalized with respect to *MICB* expression in no treatment was set as a standard. *HPRT1* was used as an internal standard. Statistical significance was determined by Student's *t*-test. $**p < 0.01$; $*p < 0.1$. HDAC, histone deacetylase; MICA/B, MHC class I polypeptide-related sequence A/B.

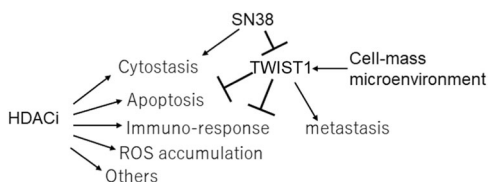


FIGURE 6 Summary of combinatorial treatment of SN38 with romidepsin.

HDACi may be one of the important benefits of the treatment. Moreover, we demonstrated that combinatorial usage of SN38 with romidepsin enhanced the MICA/B induction activity of romidepsin and allowed it to penetrate romidepsin even in cell-mass conditions, in which usage of romidepsin alone was less effective. The data suggested the HDACi efficacy on drug-resistant tumor sites, such as recurrence and metastatic lesions is worried to be spawned. However, human NKG2D ligands, namely MICA/B and ULBP1-6, are not conserved between humans and mice, due to which NK cells in mice do not recognize these molecules, and it would be limited to evaluating the substantial benefit of HDACi treatment via NK cell immune surveillance system in the xenograft animal model. Fine-tuned animal studies, such as using an NK cell-humanized mouse model, might be helpful in evaluating the substantial benefit of HDACi in SS treatment. On the other hand, the latest study reported that the HDACi Panobinostat (also known as LBH589) could enhance NK cell cytotoxicity in soft tissue sarcoma treatment [11–14] thereby suggesting that the HDACi treatment causes upregulation of both host and guest sensitivities in NK immunosurveillance system. Taken together, HDACi was considered to have great potential for suppressing SS directly as well as indirectly via the NK cell immune system. Optimized bedside studies, focused on not only direct cytotoxicity but also indirect cytotoxicity, would reveal the precise evidence of HDACi treatment for patients with SS.

Despite strong TWIST1 expression, substantial sensitivity to romidepsin was different across Yamato, SYO1, and HSSYII. One possibility for producing different responses to romidepsin is the retention of stemness. The relationship between cancer cell stemness and drug resistance is already known and upregulation of TWIST1 has been shown to link the properties through EMT in carcinoma. Yamato cells have been demonstrated to differentiate into multiple mesenchymal lineage cell types [32–35]. Consistent with that, Yamato cells showed remarkable drug resistance against romidepsin, especially in spheroid form. Furthermore, Aska cells, which have stemness without significant TWIST1 expression, did not show remarkable drug resistance even in

spheroid form. The data implied that simple TWIST1 expression was not significant for drug resistance against romidepsin. Taken together, TWIST1 expression accompanied by stemness characteristics was thought to possibly be necessary for drug resistance against romidepsin in SS cells. In the cell kinetics model of cancer chemotherapy, drug-sensitive cells are considered to be immediately killed while less sensitive cells, such as cancer stem cells, tend to survive; recurrent or metastatic sites developed from that cell population could have drug resistance, leading to difficulties in chemotherapy [48]. Therefore, declining stemness and/or TWIST1 suppression could be an important approach to overcoming drug resistance in SS treatment. Thus, the importance of SN38/irinotecan in SS treatment should be emphasized, even if it did not show significant direct cytotoxic efficacy. On the other hand, the number of Aska cells seemed to be decreased by concomitant treatment of SN38 and romidepsin, despite a weak apoptotic index judged by cleavage of Caspase3. Since HDACi has been shown to increase intracellular ROS by upregulation of NADPH oxidase activity [9], ferroptosis could be another possibility. Ferroptosis is a type of iron-dependent cell death characterized by lipid peroxide accumulation triggered by ROS. For an in-depth understanding of the entire HDACi efficacy in antitumor action, further molecular-dissection analysis would be required.

The concomitant use of multiple drugs could potentiate drug effects through a variety of mechanisms. Practically and clinically, many drugs have been tried with HDACi in lymphomas, myelomas, and several solid tumors [49]. Irinotecan, a topoisomerase I inhibitor, is one of the major conventional antitumor drugs. It has been widely applied to multiple solid tumors and is getting widespread attention recently in the treatment of pediatric sarcomas, such as Ewing sarcoma and rhabdomyosarcoma [50]. To date, there has only been little evidence of SN38/irinotecan being effective against SS. In some publications, combinatorial usage of SN38/irinotecan with HDACi in colon cancer has been reported, and the synergistic antitumor effects have been demonstrated both in vitro and in vivo [51, 52]. In the current study, we demonstrated that co-treatment with SN38 improved the efficacy of HDACi via TWIST1 suppression in SS cells. Although irinotecan/SN38 is a topoisomerase I inhibitor, whether TWIST1 is a direct target of SN38 and whether TWIST1 expression is suppressed via sumoylation, seen in topoisomerase I inhibition or other mechanisms involved, have not been dissected yet. To optimize drug efficacy, dissecting the molecular mechanisms underlying TWIST1 suppression by SN38 would be required. In another aspect, TWIST1 inhibitory activity itself represents a very important potential to suppress tumor

malignancy, besides enhancing HDACi efficacy, since TWIST1 plays a crucial role in metastasis in various tumor types. In SS, the detailed function of TWIST1 for metastasis is not well dissected yet. Given that TWIST1 is closely associated with metastasis in several types of sarcomas [53, 54], it is assumed to play a crucial role in the metastasis of SS. Thus, TWIST1 suppression by SN38 would be expected to suppress metastasis in SS as well. In that context, the metastatic loci in distant organs could be developed from TWIST1-positive cells migrated from the primary lesion through the bloodstream, suggesting the potency of drug resistance by TWIST1. Consistent with this finding, the metastatic loci are known to develop drug resistance; thus, concomitant treatment with SN38 is expected to reduce the drug resistance through TWIST1 suppression. Further study focused on metastasis inhibition with SN38 would be valuable in the future, and we plan to conduct such as study in a future project. Although TWIST1 suppression was a novel function of SN38, we tested that only in SS cell lines. To determine whether the application of SN38 is limited to SS cells or whether it can be applied to various sarcoma types, we plan to conduct a sarcoma-wide screening with cell lines and organoid lines in the future [55, 56].

Recently, drug screening with 3D culture systems has been shed light because it is thought that oversimplified cellular characteristics in the conventional 2D culture system could be more susceptible to drugs than in tumor tissues of patients. Indeed, we found severe romidepsin resistance in Yamato spheroids. TWIST1 expression was enhanced following HIF1 α stabilization, since the *TWIST1* gene is one of the direct targets of HIF1 α , indicating that more accurate drug resistance assessment would be required under 3D culture conditions, such as spheroids and tumor organoids. Of course, the conventional 2D culture system has an advantage in various situations, such as automated drug screening tests and simplicity of operation. On the contrary, the 3D culture system has disadvantages in the requirement of specific culture materials and in terms of the difficulties in cell mass preparation owing to the shortage of cell lines and lack of spheroid-forming ability in the sarcoma study field. To circumvent such limitations, various types of sarcoma organoids, including SS, are being established from patients' specimens based on sarcoma-optimized protocol [55, 56]. To accelerate the drug test and drug screening for sarcoma treatment, a combined approach of 2D and 3D culture systems would be crucial.

In this study, four SS cell lines were analyzed. Aska and Yamato cells were more resistant to romidepsin compared with SYO1 and HSSYII despite having a similar HDAC expression profile. The previous study

revealed that both Aska and Yamato cells retained stemness and the potential to differentiate into multiple cell lineages [33, 34]. Generally, the stemness and drug and apoptotic resistance are thought to be linked although their mechanisms are not fully understood [57]. Thus, the higher drug and apoptotic resistance in Aska and Yamato may be explained, in part, by the property of stemness. The four SS cell lines also showed different sensitivity against SN38. Diverse pathways are known for SN38/irinotecan resistance in tumor cells [37], but it remains unclear as to which pathway is working in SS cells. The link between stemness and higher drug resistance in tumor cells is a well-known phenomenon. As Aska and Yamato cells have been shown to have stem cell properties, the drug resistance mechanism against SN38, such as the ABCC1 transporter (also known as MRP1), may be activated in these cells.

5 | CONCLUSIONS

In conclusion, our study provided beneficial evidence of concomitant treatment of romidepsin with SN38 for SS cell treatment and discussed the concerns regarding the limitations in drug tests under 2D conditions. Application of the 3D culture system, such as spheroids and organoids, would improve drug tests for SS treatment.

AUTHOR CONTRIBUTIONS

Satoru Sasagawa: Conceptualization (lead); data curation (lead); formal analysis (lead); funding acquisition (lead); investigation (lead); methodology (lead); project administration (lead); resources (lead); supervision (lead); validation (lead); visualization (lead); writing—original draft (lead); writing—review and editing (lead). **Jun Kumai:** Conceptualization (supporting); investigation (supporting); writing—review and editing (supporting). **Toru Wakamatsu:** Conceptualization (supporting); investigation (supporting); methodology (supporting); writing—review and editing (supporting). **Yoshihiro Yui:** Conceptualization (supporting); investigation (supporting); supervision (supporting); writing—review and editing (supporting).

ACKNOWLEDGMENTS

We thank Drs. Norifumi Naka, Akira Kawai, and Hiroshi Sonobe for providing synovial sarcoma cell lines. We thank Dr. Bob Weinberg for providing the lentiviral backbone vectors via Addgene. We are grateful to members of our research institute and members of the musculoskeletal oncology group at Osaka International Cancer Institute for their valuable comments. This study

was financially supported by the Tokushukai Medical Group for the purchasing of reagents, materials, and equipment, and the preparation of the manuscript. The funders did not participate in the design of the study, data collection, analysis, or manuscript preparation.

CONFLICT OF INTEREST STATEMENT

The authors declare no conflict of interest.

DATA AVAILABILITY STATEMENT

The data that support the findings of this study are available from the corresponding author upon reasonable request.

ETHICS STATEMENT

All experiments were according to national and international guidelines and have been approved by the institutional experiments review committee (IRB) (R5-Apr-#7). No additional ethical approval was required.

INFORMED CONSENT

Not applicable.

ORCID

Satoru Sasagawa  <http://orcid.org/0000-0001-5769-8700>

Toru Wakamatsu  <http://orcid.org/0000-0002-3073-0595>

REFERENCES

1. Stacchiotti S, Van Tine BA. Synovial sarcoma: current concepts and future perspectives. *J Clin Oncol.* 2018;36(2):180–7. <https://doi.org/10.1200/JCO.2017.75.1941>
2. Gazendam AM, Popovic S, Munir S, Parasu N, Wilson D, Ghert M. Synovial sarcoma: a clinical review. *Curr Oncol.* 2021;28(3):1909–20. <https://doi.org/10.3390/curroncol28030177>
3. Kadoch C, Crabtree GR. Reversible disruption of mSWI/SNF (BAF) complexes by the SS18-SSX oncogenic fusion in synovial sarcoma. *Cell.* 2013;153(1):71–85. <https://doi.org/10.1016/j.cell.2013.02.036>
4. McBride MJ, Pulice JL, Beird HC, Ingram DR, D'Avino AR, Shern JF, et al. The SS18-SSX fusion oncoprotein hijacks BAF complex targeting and function to drive synovial sarcoma. *Cancer Cell.* 2018;33(6):1128–1141.e7. <https://doi.org/10.1016/j.ccell.2018.05.002>
5. Knott MML, Hölting TLB, Ohmura S, Kirchner T, Cidre-Aranaz F, Grünewald TGP. Targeting the undruggable: exploiting neomorphic features of fusion oncoproteins in childhood sarcomas for innovative therapies. *Cancer Metastasis Rev.* 2019;38(4):625–42. <https://doi.org/10.1007/s10555-019-09839-9>
6. Desai IME, Fleuren EDG, van der Graaf WTA. Systemic treatment for adults with synovial sarcoma. *Curr Treat Options Oncol.* 2018;19(2):13. <https://doi.org/10.1007/s11864-018-0525-1>
7. Ito T, Ouchida M, Morimoto Y, Yoshida A, Jitsumori Y, Ozaki T, et al. Significant growth suppression of synovial sarcomas by the histone deacetylase inhibitor FK228 *in vitro* and *in vivo*. *Cancer Lett.* 2005;224(2):311–9. <https://doi.org/10.1016/j.canlet.2004.10.030>
8. Lubieniecka JM, de Bruijn DRH, Su L, van Dijk AHA, Subramanian S, van de Rijn M, et al. Histone deacetylase inhibitors reverse SS18-SSX-mediated polycomb silencing of the tumor suppressor early growth response 1 in synovial sarcoma. *Cancer Res.* 2008;68(11):4303–10. <https://doi.org/10.1158/0008-5472.CAN-08-0092>
9. Laporte AN, Poulin NM, Barrott JJ, Wang XQ, Lorzadeh A, Vander Werff R, et al. Death by HDAC inhibition in synovial sarcoma cells. *Mol Cancer Ther.* 2017;16(12):2656–67. <https://doi.org/10.1158/1535-7163.MCT-17-0397>
10. Su L, Sampaio AV, Jones KB, Pacheco M, Goytain A, Lin S, et al. Deconstruction of the SS18-SSX fusion oncoprotein complex: insights into disease etiology and therapeutics. *Cancer Cell.* 2012;21(3):333–47. <https://doi.org/10.1016/j.ccr.2012.01.010>
11. Verhoeven DHJ, de Hooge ASK, Mooiman ECK, Santos SJ, ten Dam MM, Gelderblom H, et al. NK cells recognize and lyse Ewing sarcoma cells through NKG2D and DNAM-1 receptor dependent pathways. *Mol Immunol.* 2008;45(15):3917–25. <https://doi.org/10.1016/j.molimm.2008.06.016>
12. Cho D, Shook DR, Shimasaki N, Chang YH, Fujisaki H, Campana D. Cytotoxicity of activated natural killer cells against pediatric solid tumors. *Clin Cancer Res.* 2010;16(15):3901–9. <https://doi.org/10.1158/1078-0432.CCR-10-0735>
13. Klose C, Berchtold S, Schmidt M, Beil J, Smirnow I, Venturelli S, et al. Biological treatment of pediatric sarcomas by combined virotherapy and NK cell therapy. *BMC Cancer.* 2019;19(1):1172. <https://doi.org/10.1186/s12885-019-6387-5>
14. Vela M, Bueno D, González-Navarro P, Brito A, Fernández L, Escudero A, et al. Anti-CXCR4 antibody combined with activated and expanded natural killer cells for sarcoma immunotherapy. *Front Immunol.* 2019;10:1814. <https://doi.org/10.3389/fimmu.2019.01814>
15. Wu T, Dai Y. Tumor microenvironment and therapeutic response. *Cancer Lett.* 2017;387:61–8. <https://doi.org/10.1016/j.canlet.2016.01.043>
16. Arneith B. Tumor microenvironment. *Medicina.* 2019;56(1):15. <https://doi.org/10.3390/medicina56010015>
17. Gunti S, Hoke ATK, Vu KP, London Jr. NR. Organoid and spheroid tumor models: techniques and applications. *Cancers.* 2021;13(4):874. <https://doi.org/10.3390/cancers13040874>
18. Hirschhaeuser F, Menne H, Dittfeld C, West J, Mueller-Klieser W, Kunz-Schughart LA. Multicellular tumor spheroids: an underestimated tool is catching up again. *J Biotechnol.* 2010;148(1):3–15. <https://doi.org/10.1016/j.jbiotec.2010.01.012>
19. Mehta G, Hsiao AY, Ingram M, Luker GD, Takayama S. Opportunities and challenges for use of tumor spheroids as models to test drug delivery and efficacy. *J Control Release.* 2012;164(2):192–204. <https://doi.org/10.1016/j.jconrel.2012.04.045>
20. Ishiguro T, Ohata H, Sato A, Yamawaki K, Enomoto T, Okamoto K. Tumor-derived spheroids: relevance to cancer stem cells and clinical applications. *Cancer Sci.* 2017;108(3):283–9. <https://doi.org/10.1111/cas.13155>
21. Kondo J, Endo H, Okuyama H, Ishikawa O, Iishi H, Tsujii M, et al. Retaining cell-cell contact enables preparation and culture of spheroids composed of pure primary cancer cells

- from colorectal cancer. *Proc Natl Acad Sci USA*. 2011;108(15):6235–40. <https://doi.org/10.1073/pnas.1015938108>
22. Kiyohara Y, Yoshino K, Kubota S, Okuyama H, Endo H, Ueda Y, et al. Drug screening and grouping by sensitivity with a panel of primary cultured cancer spheroids derived from endometrial cancer. *Cancer Sci*. 2016;107(4):452–60. <https://doi.org/10.1111/cas.12898>
 23. Kondo J, Ekawa T, Endo H, Yamazaki K, Tanaka N, Kukita Y, et al. High-throughput screening in colorectal cancer tissue-originated spheroids. *Cancer Sci*. 2019;110(1):345–55. <https://doi.org/10.1111/cas.13843>
 24. Qin Q, Xu Y, He T, Qin C, Xu J. Normal and disease-related biological functions of Twist1 and underlying molecular mechanisms. *Cell Res*. 2012;22(1):90–106. <https://doi.org/10.1038/cr.2011.144>
 25. Zhao R, Trainor PA. Epithelial to mesenchymal transition during mammalian neural crest cell delamination. *Semin Cell Dev Biol*. 2023;138:54–67. <https://doi.org/10.1016/j.semcdb.2022.02.018>
 26. Zhu QQ, Ma C, Wang Q, Song Y, Lv T. The role of TWIST1 in epithelial-mesenchymal transition and cancers. *Tumor Biol*. 2016;37(1):185–97. <https://doi.org/10.1007/s13277-015-4450-7>
 27. Zhao Z, Rahman MA, Chen ZG, Shin DM. Multiple biological functions of Twist1 in various cancers. *Oncotarget*. 2017;8(12):20380–93. <https://doi.org/10.18632/oncotarget.14608>
 28. Yusup A, Huji B, Fang C, Wang F, Dadihan T, Wang HJ, et al. Expression of trefoil factors and TWIST1 in colorectal cancer and their correlation with metastatic potential and prognosis. *World J Gastroenterol*. 2017;23(1):110–20. <https://doi.org/10.3748/wjg.v23.i1.110>
 29. Vu T, Datta P. Regulation of EMT in colorectal cancer: a culprit in metastasis. *Cancers*. 2017;9(12):171. <https://doi.org/10.3390/cancers9120171>
 30. Fujita K, Kubota Y, Ishida H, Sasaki Y. Irinotecan, a key chemotherapeutic drug for metastatic colorectal cancer. *World J Gastroenterol*. 2015;21(43):12234–48. <https://doi.org/10.3748/wjg.v21.i43.12234>
 31. Yui Y, Itoh K, Yoshioka K, Naka N, Watanabe M, Hiraumi Y, et al. Mesenchymal mode of migration participates in pulmonary metastasis of mouse osteosarcoma LM8. *Clin Exp Metastasis*. 2010;27(8):619–30. <https://doi.org/10.1007/s10585-010-9352-x>
 32. Ishibe T, Nakayama T, Aoyama T, Nakamura T, Toguchida J. Neuronal differentiation of synovial sarcoma and its therapeutic application. *Clin Orthop Relat Res*. 2008;466(9):2147–55. <https://doi.org/10.1007/s11999-008-0343-z>
 33. Naka N, Takenaka S, Araki N, Miwa T, Hashimoto N, Yoshioka K, et al. Synovial sarcoma is a stem cell malignancy. *Stem Cells*. 2010;28(7):1119–31. <https://doi.org/10.1002/stem.452>
 34. Wakamatsu T, Naka N, Sasagawa S, Tanaka T, Takenaka S, Araki N, et al. Deflection of vascular endothelial growth factor action by SS18-SSX and composite vascular endothelial growth factor- and chemokine (C-X-C motif) receptor 4-targeted therapy in synovial sarcoma. *Cancer Sci*. 2014;105(9):1124–34. <https://doi.org/10.1111/cas.12469>
 35. Tamaki S, Fukuta M, Sekiguchi K, Jin Y, Nagata S, Hayakawa K, et al. SS18-SSX, the oncogenic fusion protein in synovial sarcoma, is a cellular context-dependent epigenetic modifier. *PLoS One*. 2015;10(11):e0142991. <https://doi.org/10.1371/journal.pone.0142991>
 36. Lee KW, Lee NK, Ham S, Roh TY, Kim SH. Twist1 is essential in maintaining mesenchymal state and tumor-initiating properties in synovial sarcoma. *Cancer Lett*. 2014;343(1):62–73. <https://doi.org/10.1016/j.canlet.2013.09.013>
 37. Kumar S, Sherman MY. Resistance to TOP-1 inhibitors: good old drugs still can surprise us. *Int J Mol Sci*. 2023;24(8):7233. <https://doi.org/10.3390/ijms24087233>
 38. Stewart SA, Dykxhoorn DM, Palliser D, Mizuno H, Yu EY, An DS, et al. Lentivirus-delivered stable gene silencing by RNAi in primary cells. *RNA*. 2003;9(4):493–501. <https://doi.org/10.1261/rna.2192803>
 39. Igarashi K, Yui Y, Watanabe K, Kumai J, Nishizawa Y, Miyaura C, et al. Molecular evidence of IGFBP-3 dependent and independent VD3 action and its nonlinear response on IGFBP-3 induction in prostate cancer cells. *BMC Cancer*. 2020;20(1):802. <https://doi.org/10.1186/s12885-020-07310-5>
 40. Skov S, Pedersen MT, Andresen L, Thor Straten P, Woetmann A, Ødum N. Cancer cells become susceptible to natural killer cell killing after exposure to histone deacetylase inhibitors due to glycogen synthase kinase-3-dependent expression of MHC class I-related chain A and B. *Cancer Res*. 2005;65(23):11136–45. <https://doi.org/10.1158/0008-5472.CAN-05-0599>
 41. Andresen L, Jensen H, Pedersen MT, Hansen KA, Skov S. Molecular regulation of MHC class I chain-related protein A expression after HDAC-inhibitor treatment of Jurkat T cells. *J Immunol*. 2007;179(12):8235–42. <https://doi.org/10.4049/jimmunol.179.12.8235>
 42. Yamanegi K, Yamane J, Kobayashi K, Kato-Kogoe N, Ohyama H, Nakasho K, et al. Sodium valproate, a histone deacetylase inhibitor, augments the expression of cell-surface NKG2D ligands, MICA/B, without increasing their soluble forms to enhance susceptibility of human osteosarcoma cells to NK cell-mediated cytotoxicity. *Oncol Rep*. 2010;24(6):1621–7. https://doi.org/10.3892/or_00001026
 43. Yang H, Lan P, Hou Z, Guan Y, Zhang J, Xu W, et al. Histone deacetylase inhibitor SAHA epigenetically regulates miR-17-92 cluster and MCM7 to upregulate MICA expression in hepatoma. *Br J Cancer*. 2015;112(1):112–21. <https://doi.org/10.1038/bjc.2014.547>
 44. Cheng GZ, Zhang W, Sun M, Wang Q, Coppola D, Mansour M, et al. Twist is transcriptionally induced by activation of STAT3 and mediates STAT3 oncogenic function. *J Biol Chem*. 2008;283(21):14665–73. <https://doi.org/10.1074/jbc.M707429200>
 45. Chien MH, Ho YC, Yang SF, Yang YC, Lai SY, Chen WS, et al. Niclosamide, an oral antihelmintic drug, exhibits antimetastatic activity in hepatocellular carcinoma cells through downregulating twist-mediated CD10 expression. *Environ Toxicol*. 2018;33(6):659–69. <https://doi.org/10.1002/tox.22551>
 46. Li H, Chen A, Yuan Q, Chen W, Zhong H, Teng M, et al. NF- κ B/Twist axis is involved in chysin inhibition of ovarian cancer stem cell features induced by co-treatment of TNF- α and TGF- β . *Int J Clin Exp Pathol*. 2019;12(1):101–12.
 47. Ni J, Ni A. Histone deacetylase inhibitor induced pVHL-independent degradation of HIF-1 α and hierarchical quality control of pVHL via chaperone system. *PLoS One*. 2021;16(7):e0248019. <https://doi.org/10.1371/journal.pone.0248019>
 48. Mansoori B, Mohammadi A, Davudian S, Shirjang S, Baradaran B. The different mechanisms of cancer drug

- resistance: a brief review. *Adv Pharm Bull.* 2017;7(3):339–48. <https://doi.org/10.15171/apb.2017.041>
49. Suraweera A, O'Byrne KJ, Richard DJ. Combination therapy with histone deacetylase inhibitors (HDACi) for the treatment of cancer: achieving the full therapeutic potential of HDACi. *Front Oncol.* 2018;8:92. <https://doi.org/10.3389/fonc.2018.00092>
50. Wagner LM. Fifteen years of irinotecan therapy for pediatric sarcoma: where to next? *Clin Sarcoma Res.* 2015;5:20. <https://doi.org/10.1186/s13569-015-0035-x>
51. Na YS, Jung KA, Kim SM, Hong YS, Ryu MH, Jang SJ, et al. The histone deacetylase inhibitor PXD101 increases the efficacy of irinotecan in *in vitro* and *in vivo* colon cancer models. *Cancer Chemother Pharmacol.* 2011;68(2):389–98. <https://doi.org/10.1007/s00280-010-1495-6>
52. Encarnação JC, Pires AS, Amaral RA, Gonçalves TJ, Laranjo M, Casalta-Lopes JE, et al. Butyrate, a dietary fiber derivative that improves irinotecan effect in colon cancer cells. *J Nutr Biochem.* 2018;56:183–92. <https://doi.org/10.1016/j.jnutbio.2018.02.018>
53. Choo S, Wang P, Newbury R, Roberts W, Yang J. Reactivation of TWIST1 contributes to Ewing sarcoma metastasis. *Pediatr Blood Cancer.* 2017;65:e26721. <https://doi.org/10.1002/psc.26721>
54. Wang S, Zhong L, Li Y, Xiao D, Zhang R, Liao D, et al. Up-regulation of PCOLCE by TWIST1 promotes metastasis in osteosarcoma. *Theranostics.* 2019;9(15):4342–53. <https://doi.org/10.7150/thno.34090>
55. Wakamatsu T, Ogawa H, Yoshida K, Matsuoka Y, Shizuma K, Imura Y, et al. Establishment of organoids from human epithelioid sarcoma with the air-liquid interface organoid cultures. *Front Oncol.* 2022;12:893592. <https://doi.org/10.3389/fonc.2022.893592>
56. Suzuki R, Wakamatsu T, Yoshida K, Matsuoka Y, Takami H, Nakai S, et al. Genetic characterization of a novel organoid from human malignant giant-cell tumor. *J Bone Oncol.* 2023;41:100486. <https://doi.org/10.1016/j.jbo.2023.100486>
57. Safa AR. Drug and apoptosis resistance in cancer stem cells (CSCs): a puzzle with many pieces. *Cancer Drug Resist.* 2022;5(4):850–72. <https://doi.org/10.20517/cdr.2022.20>

SUPPORTING INFORMATION

Additional supporting information can be found online in the Supporting Information section at the end of this article.

How to cite this article: Sasagawa S, Kumai J, Wakamatsu T, Yui Y. Improvement of histone deacetylase inhibitor efficacy by SN38 through TWIST1 suppression in synovial sarcoma. *Cancer Innov.* 2024;3:e113. <https://doi.org/10.1002/cai2.113>